

DGD Estimation from FIR Filter Taps in Presence of Higher Order PMD

F.N. Hauske (1), M. Kuschnerov (1), K. Piyawanno (1), B. Spinnler (2), E.-D. Schmidt (2), B. Lankl (1)

1 : University of the Federal Armed Forces Munich, EIT-3, 85577 Neubiberg, Germany, fabian.hauske@unibw.de

2 : Nokia Siemens Networks GmbH & Co. KG, Hofmannstr. 51, D-81379 Munich, bernhard.spinnler@nsn.com

Abstract

We estimate the DGD $\tau(\omega)$ over the complete system bandwidth from FIR filter taps in coherent receivers with digital equalization, obtaining accurate DGD values even in presence of higher order PMD.

Introduction

Optical performance monitoring (OPM) plays an important role to estimate the signal quality and derive channel parameters to control equalizer properties [1]. To reach high transmission speeds in robust optical networks, coherently demodulated polarization multiplexed (CP) QPSK has been proposed together with digital signal processing for equalization and data recovery [2]. The FIR filter, approximating the inverse channel impulse response by blind convergence [3], provides significant information about parameters such as chromatic dispersion (CD), differential group delay (DGD), OSNR [4] and even polarization dependent loss (PDL) and polarization state transformations (PST).

In [4] we showed an estimation of the DGD from FIR filter taps with $\langle \tau(\omega) \rangle$ set experimentally by a DGD emulator. In this paper we present the estimation of the DGD spectrum $\tau(\omega)$ over the complete system bandwidth with an accurate estimate of the average DGD $\langle \tau(\omega) \rangle$, even in presence of higher order PMD. We validate our results by extensive simulations.

Properties of the Filter Impulse Response

After the 90°-hybrid, the ADC and the clock recovery, we receive a digital representation of the optical field, defined in 4 dimensions with respect to the real and the imaginary part in each polarization X and Y. Operating at low channel powers, we can describe the channel as a concatenation of linear elements accumulating CD, PMD and low-pass (LP) filtering. If the equalizer (Fig. 1) is fully matched to compensate for linear channel impairments, its tap weights define the inverse of the channel impulse response.

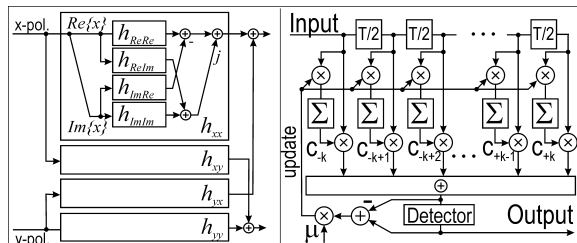


Figure 1: Complex FIR butterfly structure with exemplary real-valued implementation of h_{xx} (left) and detail of tapped delay line with filter coefficients (right)

Due to the real valued implementation, we can average over alike components to increase the accuracy

$$h_{XX} = \frac{1}{2} [(h_{XX,ReRe} + h_{XX,ImIm}) + j(h_{XX,ReIm} + h_{XX,ImIm})] \quad (1)$$

and for h_{XY}, h_{YX}, h_{YY} analogously to obtain

$$\mathbf{h} = \begin{Bmatrix} h_{XX} & h_{YX} \\ h_{XY} & h_{YY} \end{Bmatrix} \quad (2)$$

With the aid of a DFT, we compute the filter transfer function $\mathbf{H}_{\text{filt}} = DFT(\mathbf{h}) = 1/\mathbf{H}_{\text{ch}}$, which corresponds to the inverse channel transfer function.

From the literature we know

$$\mathbf{H}_{\text{filt}} = \mathbf{U}^H \cdot D^{-1} = \begin{Bmatrix} u^* & -v \\ v^* & u \end{Bmatrix} \cdot D^{-1} = \begin{Bmatrix} H_{XX} & H_{YX} \\ H_{XY} & H_{YY} \end{Bmatrix} \quad (3)$$

where \mathbf{U}^H refers to the inverse PMD matrix and D^{-1} contains the linear channel transfer function including LP filtering and the effect of CD. Neglecting PDL, we can decompose the desired transfer functions aided by the unitary property of \mathbf{U}^H with $|u|^2 + |v|^2 = 1$

$$\det(\mathbf{H}_{\text{filt}}) = D^{-2} \quad (4)$$

and

$$\mathbf{U}^H = \mathbf{H}_{\text{filt}} / D^{-1} \quad (5)$$

giving u and v . It can be shown that [5]

$$\tau(\omega) = 2\sqrt{u_\omega u_\omega^* + v_\omega v_\omega^*} = 2\sqrt{\det(\mathbf{U}_\omega)} \quad (6)$$

where $\tau(\omega)$ denotes the DGD spectrum and the index ω denotes the derivation with respect to frequency.

The digital spectral domain from $[-B, +B]$ is defined by the ADC rate of 2 samples per symbol ($B = \text{baud rate}$) with a resolution given by the number of $T/2$ spaced taps in the FIR filter. Knowing u and v , we could actually calculate back on the complete PMD vector in the Stokes space by [5]

$$\vec{\tau} = \begin{pmatrix} \tau_1 \\ \tau_2 \\ \tau_3 \end{pmatrix} = \begin{pmatrix} 2j(u_\omega u_\omega^* + v_\omega v_\omega^*) \\ 2\Im(u_\omega u + v_\omega u) \\ 2\Re(u_\omega v + v_\omega u) \end{pmatrix} \quad (7)$$

However, for realistic numbers of taps ($\# \text{taps} < 30$) the low resolution prevents accurate results.

Due to the reversed low pass filtering by the term $1/D^{-1}$, \mathbf{U}^H is degraded towards the bandwidth limits (compare fig. 3). So we confined the estimation of $\langle \tau(\omega) \rangle$ to a bandwidth of $[-0.75B, +0.75B]$ leading to an accurate estimation.

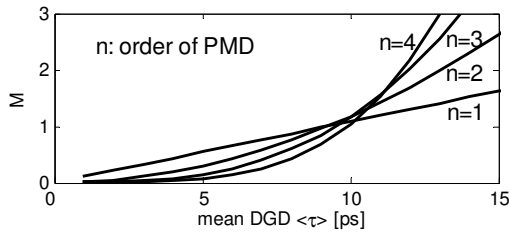


Figure 2: M_n with significant higher order PMD

Numerical Results

Simulations were carried out according to the experimental setup described in [2] with 111Gbit/s CP-QPSK (27.5 GBaud) transmitted over a linear channel with concatenated elements of PMD, CD and LP filtering. For a given mean PMD, 20 segments with randomly rotating Jones matrices in between accumulate to the total PMD. The actual $\tau(\omega)$ and $\langle \tau(\omega) \rangle$ are calculated from the resulting DGD spectrum. A complex butterfly 21-tap FIR filter bank equalizes the channel impulse response after blind convergence at OSNR=15 dB leading to BER $\approx 3 \cdot 10^{-4}$ well below the FEC limit.

For the given bandwidths, Fig. 2 shows the root mean square magnitude M_n of the first 4 orders of PMD [6].

We carried out 1000 simulations for each mean PMD of [2, 5, 10, 20, 30] ps in combination with CD ranging up to 1000 ps/nm. For CD=800 ps/nm an example of u , v , $\tau(\omega)$ and $\tau_{estim}(\omega)$ in case of $\langle \tau(\omega) \rangle = 19$ ps is given (fig. 3). For the same value of CD and a mean PMD of 20 ps, $\langle \tau_{estim}(\omega) \rangle$ vs. $\langle \tau(\omega) \rangle$ shows a precise estimation up to values of $\langle \tau(\omega) \rangle = 20$ ps, while larger values lead to a higher deviation (fig. 4).

Figure 5, which refers to a total amount of 30000 simulations, shows the standard deviation within each combination of mean PMD and CD. The estimation is robust against CD, but degrades for large values of mean PMD, where especially large values of $\langle \tau(\omega) \rangle$ above 20 ps contribute to the deviation (compare

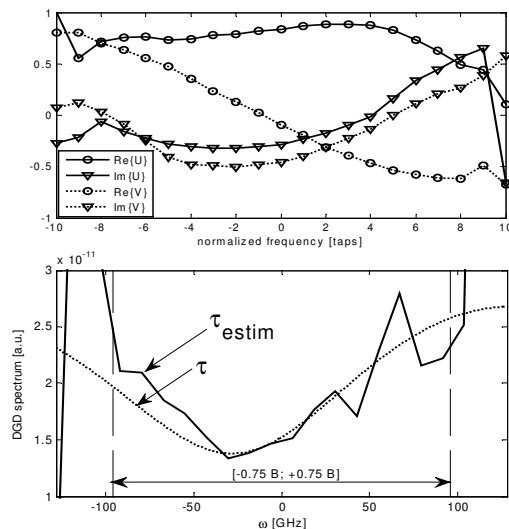


Figure 3: Example of u , v (top), $\tau(\omega)$, $\tau_{estim}(\omega)$ (bottom)

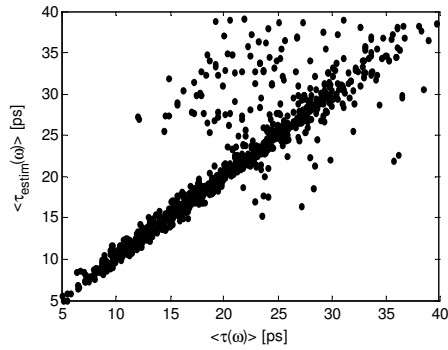


Figure 4: Estimation of $\langle \tau(\omega) \rangle$

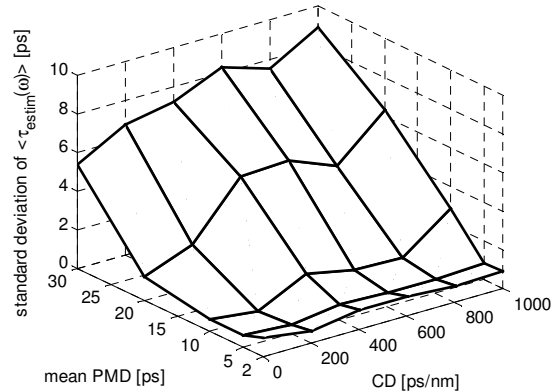


Figure 5: Standard deviation of $\langle \tau_{estim}(\omega) \rangle$ for each combination of CD and mean PMD

fig. 4). Taking into account only cases, where $\langle \tau(\omega) \rangle$ is lower than 20 ps, the standard deviation over all estimations is below 3 ps, which is highly precise. In continuous operation of FIR equalizers, the coefficient update follows polarization rotations, which vary faster than the DGD. So we receive different filter realizations for the same DGD. Thus, the estimation of large values of $\langle \tau(\omega) \rangle$ could be strongly improved by averaging over several consecutive estimations.

Conclusions

We have shown an accurate method to estimate the DGD spectrum $\tau(\omega)$ from FIR filter taps in digital equalizers of coherent receivers. Avoiding faulty samples at the bandwidth edges, we can estimate the average DGD $\langle \tau(\omega) \rangle$ precisely up to 20 ps within this bandwidth, even in presence of higher order PMD and large values of CD.

References

1. Kilper et al, JLT, Vol. 22, no. 1, (2004), p. 294
2. Fludger et al., OFC 2007, PDP22
3. Savary et al., Opt.Express 15(5), 2120-2126, 2007
4. Hauske et al. OFC 2008, OThW2
5. Gordon and Kogelnik, PNAS, Vol. 97, no. 9, (2000), p. 4541-4550
6. Shtaif and Mecozzi, *Polarisation Mode Dispersion*, Springer, New York, 2005